2026 IEEE International Conference on Robotics and Automation (ICRA 2026)
June 1-5, 2026. Vienna, Austria

Replicating Painting Strokes: Shape Aware Dynamic Motion Primitives for Robotic Manipulation

Jelena Vuletić, Pero Drobac, Bruno Marić and Matko Orsag

***Abstract*— This work proposes derivation and experimental validation of the robotic manipulation framework based on the shape aware Dynamic Motion Primitives (DMPs) that enables precise shape servoing relying on magnetic based sensing. The magnetic sensing system, with the sensor sampling rate of 1 kHz, outputs measurements that can be used as an estimate of the bending angle of the deformable plastering scraper, approximated as a constant curvature segment. Synthesized linear control algorithm encompasses PD controller that accounts for deviations in the scraper bending angle and P controller that enables maintaining end effector pitch angle reference. The proposed control system is combined with the Programming by Demonstration (PbD) approach. Consequently, the presented robotic painting system can follow the demonstrated scraper bending angle and end effector pitch angle reference values while replicating the demonstrated trajectory, even in significantly altered experimental conditions.**

I. Introduction

We present a framework for learning and reproducing painting strokes using a combination of Dynamic Motion Primitives (DMPs) and shape-based servoing, enabling robots to imitate both the motion and deformation involved in delicate artistic tasks. Painting is an ideal testbed for this challenge: It is difficult and time consuming to master, deeply personal, and requires precise control of both motion and tool deformation, characteristics shared with many delicate industrial tasks such as polishing, welding, or fine assembly. We focus on using a simple yet versatile tool — a plastering knife — which naturally introduces flexible surface interactions and soft deformation behaviors, making it an excellent fit with emerging soft robotics approaches. By targeting the nuances of stroke reproduction, we aim to push the state of the art toward robots capable of learning expressive, tool-based skills through demonstration.

Contactless robotic plastering and painting have already been extensively studied in the literature [1]. Some of the proposed solutions have even successfully enabled on-site interaction with human operators [2]. In this work, in addition to replicating human motion, our proposed robotic system also maintains contact with the surface, continuously accounting for the shape of the plastering tool. Although the state-of-the-art robotic plastering solutions that realize contact with the surface are often equipped with tools that differ significantly from the simple bendable scrapers used by humans [3], often incorporating a parallel platform that serves as an end effector [4], following the results from [5], [6], we opted for a simple deformable 3D printed scraper that enables precise shape servoing (Fig. 1). We hypothesize that, by replicating human skill, the robot can achieve comparable plastering and painting results even with such a simple tool.

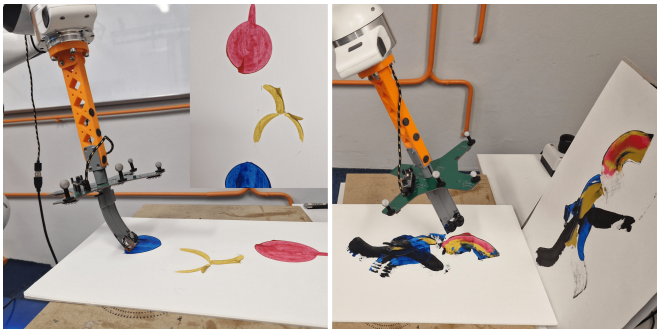

Fig. 1. Franka Emika Panda robotic manipulator, equipped with the proposed magnetic sensing system and a deformable painting scraper, drawing a simple abstract painting of a robot based on the synthetically generated trajectories (on the left). The same robotic system replicates the painting painted by a professional artist (placed vertically on the right). This is achieved using shape aware DMPs and the proposed closed-loop control system.

A. State of the art

Shape servoing of soft robots is often based on mechanical deformation models [7], with the model being generated and the deformation being simulated using the Finite-Element Method (FEM) approach [8]. Though such a model is sufficient for an open-loop control [9], some authors add an additional visual or force sensory feedback in order to improve the accuracy by closing the control loop [10]. In recent years, the focus has been on a model-free estimation of a Jacobian deformation based on sensor measurements, avoiding computationally demanding FEM analysis [11]. In most cases, the deployed proprioceptive sensors are visual [5], and often external, to avoid potential compliance deterioration [12]. In recent years, with the development of fiber optics sensing methods applicable for soft robotic applications [13], there has also been a significant number of works that propose shape servoing based on embedded optical fibers [14]. Although fiber optics sensors do possess

This work was supported in part by the project "CBRNe HERO" funded by the European Union - NextGeneration EU under Grant NPOO.C3.2.R3-I1.04.0075. The work of doctoral student Jelena Vuletić has been supported in part by the "Young researchers' career development project–training of doctoral students" of the Croatian Science Foundation funded by the European Union from the European Social Fund. The authors would also like to thank the artist Domagoj Bogdan for his patience and out-of-the-box creativity.

Authors are with LARICS Laboratory for Robotics and Intelligent Control Systems, University of Zagreb Faculty of Electrical Engineering and Computing, Unska 3, 10000 Zagreb, Croatia jelena.vuletic, pero.drobac, bruno.maric, matko.orsag @fer.unizg.hr

a number of inherent advantages, including miniature size, fast response, and light weight, their main drawback is the price, which amounts to tens of thousands of euros.

An alternative approach to shape servoing based on optical sensors is a curvature control based on magnetic sensor measurements. In this work, we follow the results from Vuletic et al. [6] that validated the application of a custom magnetic gradiometer for soft structure shape servoing. While using the same sensing setup, we significantly improved the control algorithm (Section II-B), enabling accurate replication of human motion (Section II-C), which was not feasible with the DEGAS system presented in [6]. Magnetic sensing is a cost effective, highly reliable sensing method that enables high sampling rates (our proposed system runs at 1 kHz) and consequently a seamless real-time control. Owing to that, several papers studied the possibility of a magnetic based shape servoing in soft robotics. Some of the authors opted for an external sensing array, while embedding or placing permanent magnets (PMs) onto the soft structure [15], [16]. On the contrary, we propose embedding both the sensor and the PMs, avoiding an additional calibration step. A similar approach has been adopted for soft continuum robots in [17] and [18], where an accurate shape estimation has been achieved with the learning-based method that allowed for a sampling rate of 40 Hz. In this work, we propose a system that can be as accurate, but significantly faster, achieving a sampling rate of 1 kHz and allowing for the real-time soft structure curvature control.

The synthesized linear control algorithm can be used alongside other Programming by Demonstration (PbD) systems to ensure adaptive task replication if the control input for the algorithm is demonstrated by the human operator. The movement of the human operator, together with the scraper bending angle, is memorized, and adjusted, using a well-known DMP algorithm [19], widely regarded as a stable solution for movement replication. DMP-based systems have been used as motion planning algorithms in a wide array of automation solutions, including automation of forestry cranes [20], locomotion of legged robots [21], and many more. Classic DMPs control positions for motion planning, while some tasks (such as painting or plastering) may require specific tool orientation as well. However, DMPs can be made implementation agnostic to handle rotations as separate dimensions [22]. Extending the state of the art, we propose an additional abstraction layer for recording shape that yields shape aware DMPs capable of recording the position and orientation of the tool tip alongside the shape of the tool recorded in magnetic measurements. From the replication side of the framework, we propose a novel linear control algorithm to ensure adaptive task execution.

B. Contributions

The contributions of this work are as follows:

1) We propose a robotic manipulation framework based on shape aware DMPs that enables precise curvature control relying on magnetic gradiometer measurements. The proposed system enables 1 kHz sampling rate, allowing for the seamless real-time control.
2) Shape aware DMPs enable simultaneous motion planning and shape servoing by outputting a trajectory coupled with the desired curvature of the soft structure. The demonstrated trajectories can be modified, i.e. scaled in time or space, prior to being fed to controller.
3) We present a soft robotic manipulation solution capable of maintaining the desired soft structure curvature while executing motion generated either synthetically or demonstrated by the human operator, even under conditions that significantly differ from the ones in the demonstration stage. The proposed system is experimentally validated on the robotic painting task and compared with the existing approaches.

The methodology, including the perception, control, and PbD approach, is presented in the following section. Section III outlines the experimental setup, followed by the discussion on the experimental results. Finally, Section IV concludes the paper.

II. Method

The proposed robotic system, shown in Fig. 1, consists of a Franka Emika Panda compliant robotic manipulator and a custom-designed soft end effector used as a plastering or painting scraper. The end effector encompasses a custom magnetic gradiometer, a 3D printed distancer that minimizes the influence of a rotating magnetic field generated by motors on the gradiometer measurements, and a deformable scraper with PMs mounted on the tip (Fig. 2). The scraper we propose resembles the one used by artists in plastering and painting tasks. It is a simple, 3D printed, deformable structure that can be modeled as a constant curvature (CC) segment, with the shape $\mathbf{s}(q), q \in [0, Q]$, where Q stands for the scraper curvature, allowing for a simple derivation of the kinematic model. Though a variety of formalisms can be found in the literature for a CC segment modeling, it has been shown that each of them yields the same transformation from the arc base to any point $c \in [0, D]$ of the modeled segment, with D denoting the segment length [23]. Following the results presented in [7], by simplifying the kinematic problem to two dimensions, the position of the scraper tip, that is, $c = D$, in the end effector frame L_e depends solely on the scalar curvature Q:

$$\mathbf{p}_e^D = \frac{D}{Q}\begin{bmatrix}\sin(Q) & 0 & 1-\cos(Q)\end{bmatrix}^T. \tag{1}$$

Deriving from Eq. 1, the length of the vector $\mathbf{p}_e^D$, i.e. the distance d between the root and the tip of the scraper, can be directly obtained if the scraper curvature Q is known:

$$d = \frac{D}{Q}\sqrt{2\cdot(1-\cos(Q))}. \tag{2}$$

Consequently, the difference between the commanded and the actual scraper curvature Q, indirectly measured with the custom magnetic gradiometer, as discussed in Section II-A, can be compensated by adjusting the distance d. The adjustment is realized with the implemented linear control system

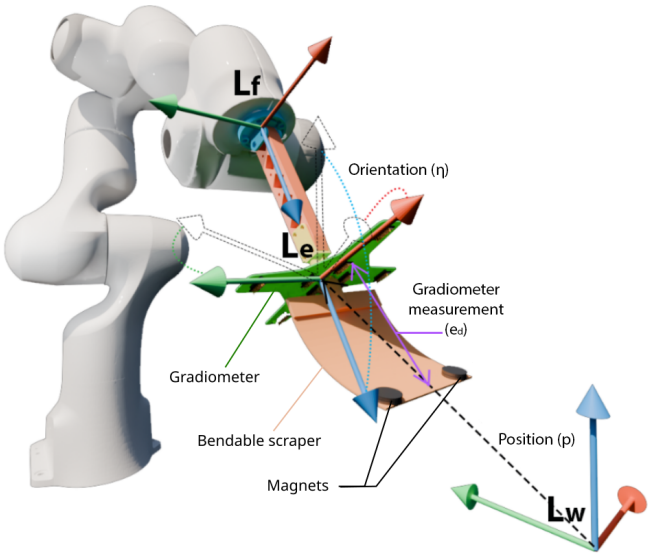

Fig. 2. Robotic manipulation based on shape aware DMPs encompasses shape estimation based on magnetic gradiometer measurements e_d and position and orientation tracking of the end effector frame L_e in the world frame L_w with either OptiTrack motion capture system (when human operator demonstrates the movement) or based on the robot kinematics.

(Section II-B) that allows for smooth reference tracking, even when using an output from the shape aware DMP algorithm as a reference (Section II-C).

A. Proprioceptive sensing

The proposed method for shape aware motion replication requires both the scraper shape deformation estimation and scraper movement tracking (Fig. 2). The shape of the scraper, i.e. its curvature Q, is approximated based on the custom magnetic sensor. Though magnetic based sensing is accurate, precise, and fast, it often suffers form the influence of the Earth's magnetic field. To mitigate that problem, following the results from [24], in this work, we measure the magnetic tensor components instead of the magnetic flux. The measurement is conducted using a custom magnetic gradiometer and relying on the scalar ranging with improved orientation detection (SRIOD) method. Additional details on both the gradiometer and SRIOD method can be found in [25].

The deployed gradiometer encompasses eight equally oriented 3-axial magnetometers. Based on the individual measurements of magnetometers, gradient tensor contractions (GTCs), a compact representation of the measured magnetic field gradient's magnitude, are calculated. To estimate the distance between the root and the tip of the scraper, we rely on measurements of the outer four magnetometers. First, partial contractions of the outer sensor pairs are calculated as follows:

$$C_{Pij} = \sqrt{\frac{1}{{L_{ij}}^2}(\vec{B}_i - \vec{B}_j)^T(\vec{B}_i - \vec{B}_j)} \quad (i,j) \in \{(3,4),(0,7)\}, \tag{3}$$

with L denoting the distance between the sensors and $\vec{B}$ the magnetic gradient of the PM. The partial contractions of the outer sensor pairs, C_{P34} and C_{P07} are used as an estimate of the distance d between the root and the tip of the scraper:

$$e_d = C_{P34} + C_{P07}. \tag{4}$$

This estimate is not accurate absolute distance estimation, instead it outputs a raw value that decreases as the distance is reduced, so for simplicity's sake it will be referred to as the gradiometer measurement going forward.

However, in order to mimic the motion of the human operator, it is crucial to keep track of not only the scraper shape, i.e. the gradiometer measurement e_d, but also the movement of the scraper itself. For that reason, motion capture reflective markers are placed along the gradiometer and the accompanying 3D printed distancer. Using the OptiTrack motion capture system, we were able to accurately record both the position and the orientation of the proposed painting tool when held by the human operator.

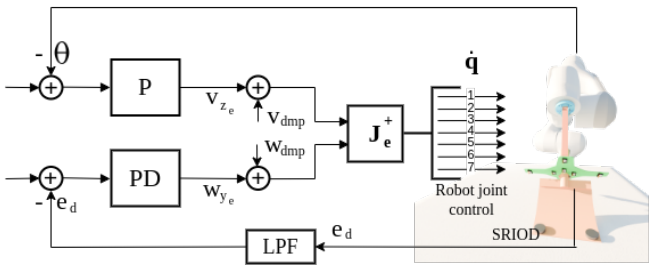

Fig. 3. The proposed control algorithm encompasses PD controller that accounts for deviations in the scraper bending angle by rotating the robot end effector around its y-axis and P controller that regulates the robot end effector angle by translating the robot end effector around its z-axis. The outputs from the controllers, i.e. linear and angular velocities, are summed with the velocities generated by the shape aware DMP.

B. Control

With the deployed 7 DOF manipulator, the compensation of the scraper curvature Q error can be done either by modifying the robot end effector pitch angle (rotation around the y-axis of the end effector frame L_e), or by translating the end effector frame along the z-axis of the same frame (Fig. 2). Consequently, the deformation of the plastering scraper approximated as a constant curvature segment at the arc point $c = D$ for the curvature Q is defined as:

$$\dot{\mathbf{s}}(Q) = \mathbf{J}_o(\mathbf{s}(Q)) \cdot \begin{bmatrix} v_{z_e} \\ w_{y_e} \end{bmatrix}, \tag{5}$$

where $\mathbf{J}_o(\mathbf{s}(Q))$ denotes the deformation Jacobian at the current shape $\mathbf{s}(Q)$ and $\mathbf{v}_{z_e}$ and $\mathbf{w}_{y_e}$ denote the outputs from the controllers (Fig. 3).

In [6], a classic PD approach was adopted to minimize the scraper curvature error by translating the robot end effector along the z-axis. As the robot's pitch angle wasn't taken into consideration in [6], the gradiometer could potentially collide with the inclined surface. For that reason, we propose compensating the scraper curvature error by controlling both the y-axis rotation and the z-axis translation of the end effector frame. While minimizing the safety risk, the proposed

approach also allows us to simultaneously account for the smooth adjustments and to compensate for the larger errors caused by irregular surfaces. Additionally, by incorporating the rotation into the control algorithm, we gain an additional control input, allowing us to keep the robot's pitch angle either at the constant reference value or to replicate the same pitch angle used by a human operator during plastering and painting tasks (Section II-C). Though the work of Vuletic et al. [6] enabled for certain level of autonomous robotic painting, the lack of additional control input prevented the possibility of an accurate human motion replication based on the proposed shape aware DMPs. Motivated by that, in this work we synthesized a linear closed-loop control algorithm, shown in Fig. 3. System identification was conducted prior to control design using *MATLAB System Identification Toolbox*. Parameters of an open-loop transfer functions are identified based on a known input velocity signal and a specified curvature Q, using a low-amplitude sine-wave velocity input.

The system is controlled at 1 kHz with the gradiometer measurements being provided at the same rate. Relying on Eq. 2 and Eq. 5, the gradiometer measurements function $e_d(d)$ can be linearized allowing for the implementation of the linear control algorithm:

$$\Delta e_d = \mathbf{J}_g(\mathbf{s}(Q)) \cdot \dot{\mathbf{s}}(Q), \tag{6}$$

with $\mathbf{J}_g(\mathbf{s}(Q))$ denoting the gradiometer measurement Jacobian at the current shape $\mathbf{s}(Q)$. Due to the high sampling rate, the measurements encompass noise filtered using a low-pass filter with a cutoff frequency of 100 Hz. The PD controller (Fig. 3), with tuned parameters amounting to 10^{-7} and 10^{-12} for proportional and derivative gain, respectively, takes the distance estimate e_d as an input (Eq. 4) and manipulates the robot rotation around the y-axis of the robot end effector (robot pitch angle). The current robot pitch angle, as well as the reference value, are used as inputs for the P controller that manipulates the robot position along the z-axis of the robot end effector. Tuned proportional gain of the P controller amounts to 0.02. Both controllers are implemented as joint velocity controllers.

Based on the outputs of the controllers, a linear $\vec{\mathbf{v}}_{z_e} = v_{z_e} \cdot \hat{\mathbf{z}}_e$ and an angular $\vec{\mathbf{w}}_{y_e} = w_{y_e} \cdot \hat{\mathbf{y}}_e$ velocity vector in the z-direction and the y-direction of the robot end effector, respectively, are generated. Linear $\vec{\mathbf{v}}_{dmp}$ and angular $\vec{\mathbf{w}}_{dmp}$ velocity vectors represent either synthetically generated or demonstrated robot trajectories. Finally, the joint velocities $\dot{\vec{\mathbf{q}}}$ are calculated by taking the pseudoinverse of the Jacobian matrix:

$$\dot{\vec{\mathbf{q}}} = \mathbf{J}_e^{+} \begin{bmatrix} \vec{\mathbf{v}}_{z_e} + \vec{\mathbf{v}}_{dmp} \\ \vec{\mathbf{w}}_{y_e} + \vec{\mathbf{w}}_{dmp} \end{bmatrix}. \tag{7}$$

By using the pseudoinverse of the Jacobian matrix instead of the inverse of the reduced Jacobian matrix, as it was done in [6], we avoid reducing the robot dexterity. Consequently, the robotic manipulator is able to execute more complex trajectories. The resulting joint velocities $\dot{\vec{\mathbf{q}}}$ are sent to the internal joint impedance controller of the Franka manipulator.

C. Shape aware DMP

DMPs function as linear point attractors based on a dampened spring with an added non-linear forcing term, which gives them their shape:

$$\tau^2 \ddot{\vec{\mathbf{p}}} = \alpha_z(\beta_z(\vec{\mathbf{g}} - \vec{\mathbf{p}}) - \tau\dot{\vec{\mathbf{p}}}) + \vec{\mathbf{f}}, \tag{8}$$

where τ is the execution time of the whole operation, $\mathbf{p}$ is the current position vector, $\mathbf{g}$ is the goal position vector, α_z and β_z are dampened spring constants and $\mathbf{f}$ is the nonlinear forcing term. In order to replicate a given tool trajectory, the forcing term can be defined using weighted Gaussian radial basis functions (RBFs)

$$\vec{\mathbf{f}} = \frac{\sum_{i=1}^{N} \vec{\boldsymbol{\psi}}_i \vec{\mathbf{w}}_i}{\sum_{i=1}^{N} \vec{\boldsymbol{\psi}}_i}, \tag{9}$$

where $\boldsymbol{\psi}_i$ represents a single Gaussian RBF and w_i is the weight matching each RBF. Using a given trajectory (demonstration), this system can calculate the weights necessary to replicate it using linear regression. After calculating the weights, this system can be used to replicate the stroke motion even with different start and goal positions, meaning the task can be replicated elsewhere. While often parametrized over time, DMPs can be parametrized over phase by deriving $\mathbf{p}$ over the phase variable instead of time to allow temporal scalability during replication. This will prove vital for the replication phase, where slowing down the stroke execution allows the control framework to execute it precisely.

Given that DMPs function as point attractors with an additional forcing term, they can include any parameter with start and end values. For that reason, we can to expand the position vector $\mathbf{p}$ as an abstract state vector $\boldsymbol{\chi}$ that includes the positions $\mathbf{p}$, orientations as Euler angle values $\boldsymbol{\eta}$, and the reference value of the gradiometer measurement e_d - all provided for the proposed control algorithm:

$$\vec{\boldsymbol{\chi}} = \left(\vec{\mathbf{p}},\ \vec{\boldsymbol{\eta}},\ e_d\right)^T. \tag{10}$$

The components of the state vector $\boldsymbol{\chi}$ are visualized in Fig. 2.

This way of defining orientation faces the standard Euler angle representation problem - i.e, multiple angle triplets can describe the same orientation. This is solved by generating multiple roll, pitch, and yaw triplet candidates for each pose's orientation during both demonstration and replication. At each sample time we select the candidate most similar to the previous pose's roll, pitch, and yaw angles, thus numerically solving ambiguity. The demonstrated trajectory can then be converted to an array of poses with shape encoded as gradiometer measurements e_d to yield shape aware DMP. Image c) in Fig. 4 displays segmented demonstration trajectories which can be replicated by the shape aware DMP. Due to physical limitations of the robot, i.e. joint velocity limits amounting to 2.175 rad/s for the first four joints of the Franka Emika Panda robotic manipulator, the phase parametrized DMP variant was used to scale the execution time with the factor 10 to slow down the replication velocity and ensure accuracy. Since demonstrated trajectories are noisy

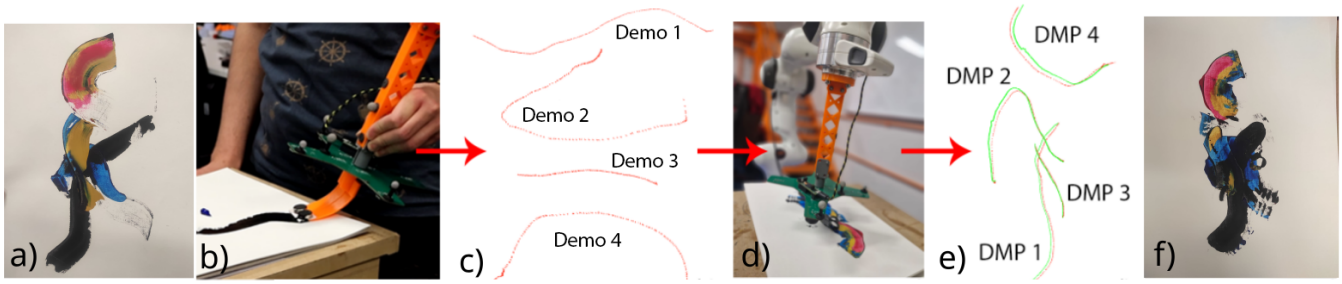

Fig. 4. The shape aware DMP pipeline deployed for the collaborative robotic painting task. A professional artist demonstrates the movement (b), separated in four distinct shapes all learned and displayed individually from different angles (c). Robotic manipulator replicates the scraper movement while maintaining demonstrated scraper curvature (d) in correct relative poses, creating a painting (f) that successfully replicates the image painted by a professional artist (a). Overlap of the demonstrated (red) and executed (green) trajectories is shown in subfigure e).

due to imprecise measurements, the shape aware DMP output is smoothed using a moving average smoothing algorithm where the moving window includes 0.5 seconds of measurements.

The smoothed trajectory must now be converted to reference values for the control algorithm. Alongside e_d, the control algorithm uses linear and angular velocities as described in Eq. 7. For the final step, the resulting shape aware DMP trajectory (excluding the magnet sensor reference value) is derived over time to output linear and angular velocities, which are summed with equivalent velocities generated by the control algorithm based on the magnet sensor reference values (e_d):

$$\vec{\mathbf{v}}_{dmp} = \dot{\vec{\mathbf{p}}}, \vec{\mathbf{w}}_{dmp} = \dot{\vec{\boldsymbol{\eta}}}. \tag{11}$$

III. Experimental Validation

The proposed control algorithm is implemented in the ROS environment and validated on the robotic painting task. First, the robotic painting system is put to test in an ablation study where a simple linear stroke was demonstrated by a human operator and repeated with and without the proposed manipulation framework. Following that, the proposed system is tasked with drawing paintings with the constant reference values and synthetically generated trajectories. As the next step, the constant reference values are replaced with the reference values demonstrated by the human operator. Additionally, the same task is executed under altered conditions, demonstrating robustness of the proposed approach. The results, in terms of trajectory RMSE and shape servoing accuracy, are reported and compared with the existing approaches.

A. Ablation study

Initial experiments are conducted on the replication of a simple linear stroke, shown in Fig. 5. The stroke was demonstrated by a human operator, with 1 mL of acrylic paint placed on the predefined position. Afterwards, the stroke was replicated by the proposed robotic system, first while maintaining the constant scraper bending angle and then by replicating the demonstrated bending angle during the entire trajectory with the proposed shape aware DMPs. In both cases, the same amount of paint was placed on the same position, the initial pose of the robot was the same, and the trajectory was identical to the demonstrated one. Considering that the accuracy of the replication is highly dependent on the initial bending angle of the scraper and in order to ensure fair comparison, when replicating the stroke with the constant reference value the reference was equal to the initial scraper bending angle that the human operator demonstrated. The results of the shape servoing are shown in Fig. 6.

The overlap of the original stroke and the replicated ones is calculated as intersection over union (IoU), amounting to 0.57 for the IoU of the original stroke and replication with the constant reference value, and 0.72 for the IoU of the original stroke and the replication with the demonstrated reference value. The intersection area percentage of almost 70% between the stroke replicated with the proposed approach and the demonstrated one, when compared to 55% for the stroke with the constant reference value, clearly demonstrates the benefits of the proposed method, even in such a simple scenario (Fig. 5).

B. Synthetically generated trajectories

In order to validate the proposed control algorithm in more complex use case, the linear and angular velocity vectors that result in linear and circular robot trajectories are generated. The control algorithm was given constant scraper bending angle and robot end effector pitch angle reference values. The output from the controller was summed with the generated velocities, resulting in the robotic manipulator executing predefined linear and circular trajectories while successfully maintaining constant scraper bending angle and robot end effector pitch angle (Fig. 7). Consequently, the robotic painting system was able to generate various abstract images (Fig. 1).

C. Demonstrated trajectories

Following the initial experiments in which the synthesized control algorithm was validated, the proposed robotic manipulation framework based on shape aware DMPs was also tested out on a robotic painting task. A professional artist was tasked with creating a painting using the deformable scraper, paint and a small number of strokes while the scraper shape and pose were being recorded, as discussed in Section II-A.

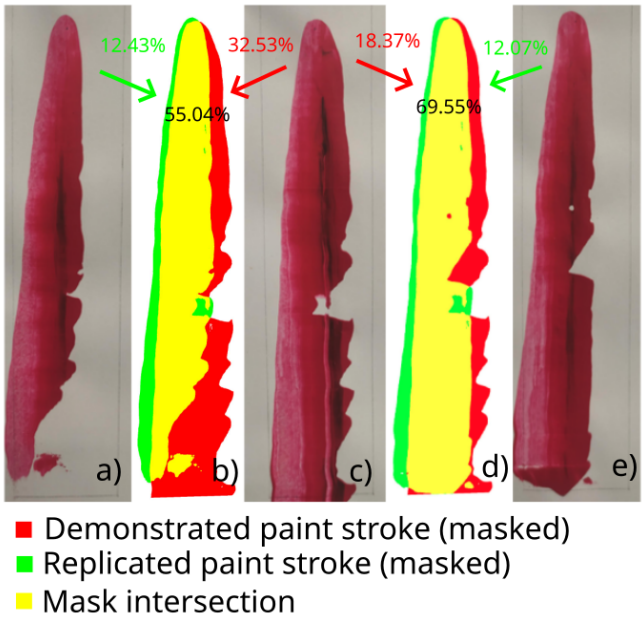

Fig. 5. Intersection comparison of the demonstrated stroke (c), replication with constant scraper angle (a) and shape aware replication (e). Intersection of (a) and (c) is shown in (b) and intersection of (c) and (e) is shown in (d). The area percentage of each color is shown near the top of the image (red for the demonstrated stroke, green for the replicated stroke, yellow/black for their intersection).

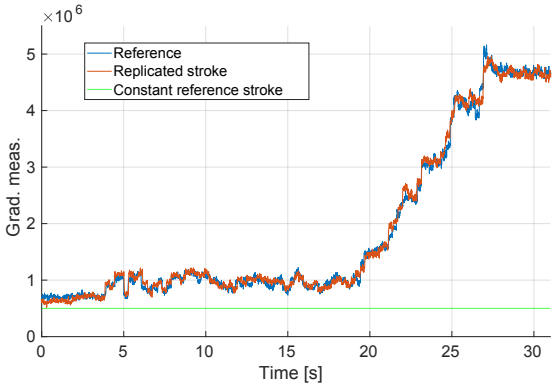

Fig. 6. Demonstrated scraper bending angle reference for a simple linear stroke along with the executed values recorded during the stroke replication with the proposed robotic system. For comparison, the same stroke is also executed with the constant reference value of $5e^5$ (see also Fig. 5).

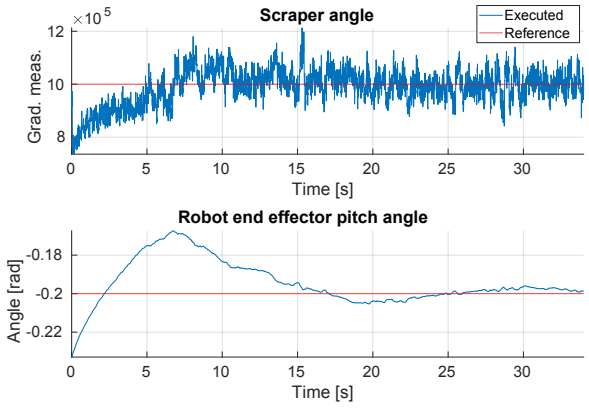

Fig. 7. Reference and recorded executed values for both the scraper bending angle and the robot end effector pitch angle while executing predefined linear and circular trajectories.

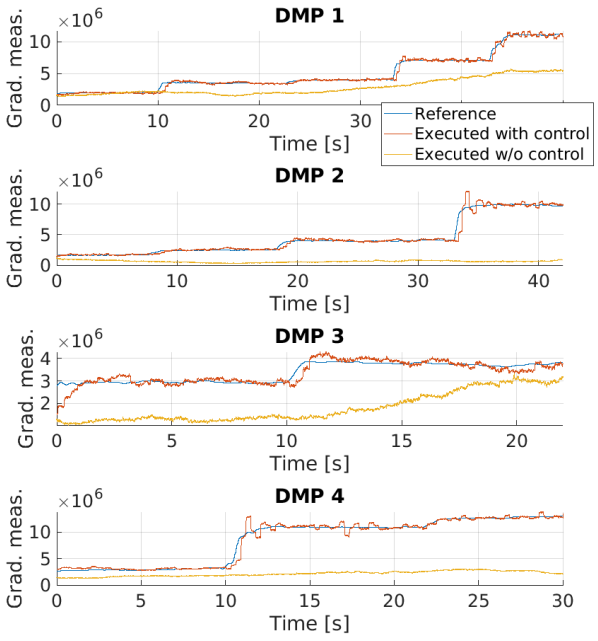

Fig. 8. Reference and recorded executed values for the scraper bending angle while executing motion demonstrated by a professional artist with the proposed robotic manipulation framework on the flat surface (see also Fig. 4). Executed scraper bending angle values recorded when replicating the trajectory without the additional shape servoing are also shown for comparison.

Afterwards, the recorded strokes were replicated using three different control variants: pure trajectory replication without the additional shape servoing (*basic DMP*), the control approach presented in [6] (*DEGAS*) and the proposed control algorithm that incorporates shape aware DMPs. Prior to replication, velocities were scaled due to joint velocity limits of the robotic manipulator, allowing for smooth robot control without deteriorating the resulting trajectory. The root mean squared error (RMSE), calculated for each of the four demonstrated movements shown in Fig. 4, is used as an accuracy metrics and represents deviation of the executed trajectories from the trajectory demonstrated by the human operator (Table I). The accuracy of the shape servoing, reported in Table II, is calculated using the mean absolute percentage error (MAPE) of the gradiometer distance measurement, as a representation of the deviation of the executed scraper angle $e_d^{(\text{exec})}$ from the scraper angle demonstrated by the human operator $e_d^{(\text{demo})}$ for N measurements:

$$Accuracy = 100\% - \frac{100\%}{N}\sum_{i=1}^{N}\left|\frac{e_{d_i}^{(\text{demo})} - e_{d_i}^{(\text{exec})}}{e_{d_i}^{(\text{demo})}}\right|. \quad (12)$$

As expected, the accuracy of the shape servoing with the *basic DMP* approach, as visible from both Table II

TABLE I

RMSE CALCULATED AS THE DEVIATION OF THE EXECUTED TRAJECTORY FROM THE TRAJECTORY DEMONSTRATED BY THE HUMAN OPERATOR FOR FOUR DISTINCT MOVEMENTS SHOWN IN FIG. 4.

	DMP1	DMP2	DMP3	DMP4
basic DMP	0.000708	0.000750	0.001189	0.001020
DEGAS [6]	0.003650	-	0.001943	-
ours	0.001733	0.002466	0.001274	0.001639

TABLE II

SHAPE SERVOING ACCURACY FOR FOUR DISTINCT MOVEMENTS SHOWN IN FIG. 4.

	DMP1	DMP2	DMP3	DMP4
basic DMP	59.69%	15.56%	54.19%	32.06%
DEGAS [6]	95.18%	-	90.02%	-
ours	92.84%	94.12%	90.31%	92.52%

and Fig. 8, is unsatisfactory. It is important to note that, without the additional control, the scraper shape is formed by external factors, such as surface irregularities. Consequently, when sliding along irregular surfaces, the *basic DMP* approach cannot ensure that the scraper remains in contact with the surface. However, as there is no additional shape servoing control algorithm that would introduce disturbances into trajectory reference tracking, the *basic DMP* approach can replicate the demonstrated trajectory with the smallest RMSE.

The *DEGAS* framework, incorporating the scraper bending angle control, can reach high shape servoing accuracy. Nevertheless, it allows for successful replication of only two out of four movements demonstrated by the human operator. The movements which could not have been executed, DMP2 and DMP4, required dexterity level which could not be reached by controlling only six joints of the Franka Emika Panda manipulator, as it was implemented in the *DEGAS* framework.

Finally, our proposed approach based on the joint translational and rotational control approach, with the addition of shape aware DMPs, can accurately replicate the demonstrated trajectories while following the demonstrated magnetic sensor reference values and consequently maintaining the desired scraper bending angle (Fig. 8). The comparison of the demonstrated stroke trajectories with the replicated trajectories executed by the robotic manipulator is shown in Fig. 4.

The proposed robotic painting system based on shape aware DMPs was able to successfully replicate the painting generated by the artist (Fig. 1). It is important to note that the paint was manually placed on the canvas prior to replicating the strokes, causing slight differences between the original and the replicated painting. However, even with the velocities being significantly scaled compared to the demonstrated ones, with the scaling factor amounting to 0.1, and considering that demonstrated scraper bending angle encompassed multiple sudden changes in the reference value (Fig. 8) and the demonstrated movement required significant change in the tool orientation (DMP2 in Fig. 4), the robotic manipulation framework based on shape aware DMPs was able to successfully replicate the demonstrated painting strokes.

TABLE III

TRAJECTORY RMSE FOR THE PROPOSED APPROACH UNDER ALTERED CONDITIONS.

	DMP1	DMP2	DMP3	DMP4
concave surface	0.003717	0.003025	0.001555	0.001767
scaled trajectory	0.001271	0.002400	0.000553	0.001724

TABLE IV

SHAPE SERVOING ACCURACY FOR THE PROPOSED APPROACH UNDER ALTERED CONDITIONS.

	DMP1	DMP2	DMP3	DMP4
concave surface	92.90%	93.65%	87.86%	87.17%
scaled trajectory	95.20%	94.55%	91.80%	87.97%

D. Demonstrated trajectories under altered conditions

After successfully validating the proposed robotic manipulation framework on the robotic painting task, the system is deployed under altered external conditions, i.e. the flat surface is replaced with the irregular one, followed by the experiment with the altered reference input, i.e. spatially scaled trajectories. Both the trajectory RMSE (Table III) and shape servoing accuracy (Table IV) are reported for both cases.

First, the flat surface on which the movements were demonstrated is replaced with the irregular, concave surface. As the robotic system is not *a priori* aware of the surface irregularities, its control algorithm has to be able to adjust the scraper bending angle in real-time in order to successfully replicate the demonstrated painting strokes. In this experiment, it was shown that the shape servoing accuracy, reported in Table IV and also visible in Fig. 9, remains sufficiently high even in such challenging conditions. Trajectory RMSE, reported in Table III, is somewhat lower than for the flat surface (Table I). This is expected as the surface irregularities necessarily alter the pose of the end effector.

The proposed framework based on shape aware DMPs was also validated to be invariant to scale. Given goal poses that are half as far from the starting pose as the original goal pose of each trajectory, the system is tested with performing trajectories that are half as long. To properly validate the execution, the output trajectories are compared to demonstrated trajectories that have been scaled by the same factor. Trajectory RMSE (Table III) for all of the demonstrated movements remained as low as for the trajectories that were not scaled (Table I). Shape servoing accuracy (Table II) was also unchanged, except for DMP4 that required significant rotation of the end effector. Spatially scaling such movement introduced imperfections in the scraper bending angle reference tracking.

IV. CONCLUSION

Motivated by the fact that humans, unlike state-of-the-art autonomous robotic painting and plastering systems, use simple, deformable scrapers for the aforementioned tasks, this work proposes a novel method based on shape aware DMPs

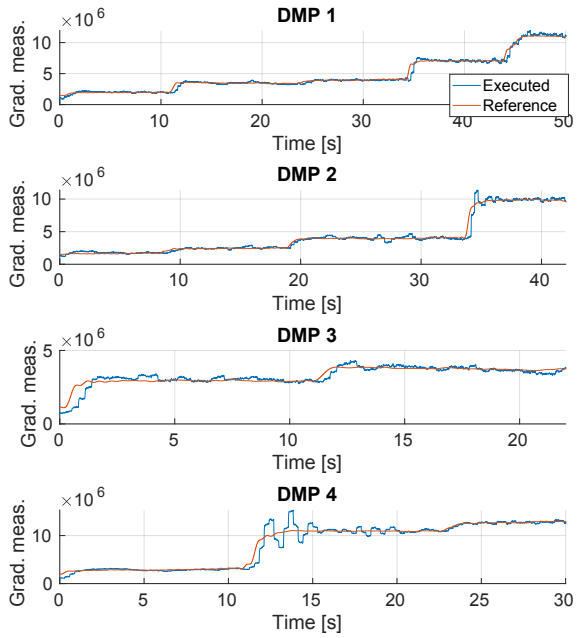

Fig. 9. Reference and recorded executed values for the scraper bending angle while executing motion demonstrated by a professional artist with the proposed robotic manipulation framework on the concave surface.

for robotic manipulation validated on the robotic painting task. The proposed method incorporates magnetic based proprioceptive sensing system working at the frequency of 1 kHz and consequently allowing for the real-time control. The synthesized linear control system encompasses two separate control loops for rotational and translational movement resulting in a smooth reference tracking for both the constant reference values and reference values demonstrated by the human operator. Finally, combining PbD approach with the proposed shape servoing method enables accurate replication of the demonstrated movement even in altered scenarios and yields significantly better results compared to the existing approaches when tested on the robotic painting task.

REFERENCES

[1] C. Okonkwo and T. Sulbaran, "A review of commercially available autonomous painting robots in the construction industry," *EPiC Series in Built Environment*, vol. 5, pp. 514–522, 2024.

[2] D. Mitterberger, S. Ercan Jenny, L. Vasey, E. Lloret-Fritschi, P. Aejmelaeus-Lindström, F. Gramazio, and M. Kohler, "Interactive robotic plastering: Augmented interactive design and fabrication for on-site robotic plastering," in *Proceedings of the 2022 CHI Conference on Human Factors in Computing Systems*, CHI '22, (New York, NY, USA), Association for Computing Machinery, 2022.

[3] X. Li and X. Jiang, "Development of a robot system for applying putty on plastered walls," in *2018 IEEE International Conference on Mechatronics and Automation (ICMA)*, pp. 1417–1422, IEEE, 2018.

[4] Z. Liu, D. Chen, M. A. Eldosoky, Z. Ye, X. Jiang, Y. Liu, and S. S. Ge, "Puttybot: A sensorized robot for autonomous putty plastering," *Journal of Field Robotics*, vol. 41, no. 6, pp. 1744–1764, 2024.

[5] M. Polic, B. Maric, and M. Orsag, "Soft robotics approach to autonomous plastering," in *2021 IEEE 17th International Conference on Automation Science and Engineering (CASE)*, pp. 482–487, 2021.

[6] J. Vuletić, B. Marić, and M. Orsag, "Degas - deformation estimation based on magnetic gradient tensor contraction for soft robot shape servoing," in *2025 IEEE 8th International Conference on Soft Robotics (RoboSoft)*, pp. 1–6, 2025.

[7] C. Della Santina, C. Duriez, and D. Rus, "Model-based control of soft robots: A survey of the state of the art and open challenges," *IEEE Control Systems Magazine*, vol. 43, no. 3, pp. 30–65, 2023.

[8] C. Armanini, F. Boyer, A. T. Mathew, C. Duriez, and F. Renda, "Soft robots modeling: A structured overview," *IEEE Transactions on Robotics*, vol. 39, no. 3, pp. 1728–1748, 2023.

[9] F. Ficuciello, A. Migliozzi, E. Coevoet, A. Petit, and C. Duriez, "Fem-based deformation control for dexterous manipulation of 3d soft objects," in *2018 IEEE/RSJ International Conference on Intelligent Robots and Systems (IROS)*, pp. 4007–4013, 2018.

[10] J. Sanchez, K. Mohy El Dine, J. A. Corrales, B.-C. Bouzgarrou, and Y. Mezouar, "Blind manipulation of deformable objects based on force sensing and finite element modeling," *Frontiers in Robotics and AI*, vol. 7, 2020.

[11] M. Shetab-Bushehri, M. Aranda, Y. Mezouar, and E. Özgür, "As-rigid-as-possible shape servoing," *IEEE Robotics and Automation Letters*, vol. 7, no. 2, pp. 3898–3905, 2022.

[12] F. Xu, Y. Zhang, J. Sun, and H. Wang, "Adaptive visual servoing shape control of a soft robot manipulator using bézier curve features," *IEEE/ASME Transactions on Mechatronics*, vol. 28, no. 2, pp. 945–955, 2023.

[13] K. C. Galloway, Y. Chen, E. Templeton, B. Rife, I. S. Godage, and E. J. Barth, "Fiber optic shape sensing for soft robotics," *Soft Robotics*, vol. 6, no. 5, pp. 671–684, 2019. PMID: 31241408.

[14] B. Mao, K. Zhou, Y. Xiang, Y. Zhang, Q. Yuan, H. Hao, Y. Chen, H. Liu, X. Wang, X. Wang, and J. Qu, "A bioinspired robotic finger for multimodal tactile sensing powered by fiber optic sensors," *Advanced Intelligent Systems*, vol. 6, no. 8, p. 2400175, 2024.

[15] S. Song, H. Ge, J. Wang, and M. Q.-H. Meng, "Real-time multi-object magnetic tracking for multi-arm continuum robots," *IEEE Transactions on Instrumentation and Measurement*, vol. 70, pp. 1–9, 2021.

[16] G. Pittiglio, A. Donder, and P. E. Dupont, "Continuum robot shape estimation using magnetic ball chains," 2024.

[17] C. F. R. Costa and J. C. P. Reis, "End-point position estimation of a soft continuum manipulator using embedded linear magnetic encoders," *Sensors*, vol. 23, no. 3, 2023.

[18] T. Baaij, M. Klein Holkenborg, M. Stoelzle, D. Tuin, J. Naaktgeboren, R. Babuska, and C. Della Santina, "Learning 3d shape proprioception for continuum soft robots with multiple magnetic sensors," *Soft Matter*, vol. 19, 12 2022.

[19] A. J. Ijspeert, J. Nakanishi, and S. Schaal, "Movement imitation with nonlinear dynamical systems in humanoid robots," in *Proceedings 2002 IEEE International Conference on Robotics and Automation (Cat. No. 02CH37292)*, vol. 2, pp. 1398–1403, IEEE, 2002.

[20] P. La Hera, D. O. Morales, and O. Mendoza-Trejo, "A study case of dynamic motion primitives as a motion planning method to automate the work of forestry cranes," *Computers and Electronics in Agriculture*, vol. 183, p. 106037, 2021.

[21] W. Ubellacker, N. Csomay-Shanklin, T. G. Molnar, and A. D. Ames, "Verifying safe transitions between dynamic motion primitives on legged robots," in *2021 IEEE/RSJ International Conference on Intelligent Robots and Systems (IROS)*, pp. 8477–8484, 2021.

[22] B. Nemec, F. J. Abu-Dakka, B. Ridge, A. Ude, J. A. Jørgensen, T. R. Savarimuthu, J. Jouffroy, H. G. Petersen, and N. Krüger, "Transfer of assembly operations to new workpiece poses by adaptation to the desired force profile," in *2013 16th International Conference on Advanced Robotics (ICAR)*, pp. 1–7, IEEE, 2013.

[23] R. J. W. III and B. A. Jones, "Design and kinematic modeling of constant curvature continuum robots: A review," *The International Journal of Robotics Research*, vol. 29, no. 13, pp. 1661–1683, 2010.

[24] D. Martinović and M. Orsag, "Magnetic flux servoing for precise localization based on gradient tensor contractions," in *2023 IEEE 19th International Conference on Automation Science and Engineering (CASE)*, pp. 1–6, 2023.

[25] D. Martinović, J. Vuletić, D. Stuhne, M. Orsag, and Z. Kovačić, "Object localization by construction of an asymmetric isobody of the magnetic gradient tensor contraction using two identical permanent magnets," *IEEE Transactions on Magnetics*, vol. 59, no. 4, pp. 1–9, 2023.